AN ALGORITHM FOR ELIMINATING THE DUODECAPOLE COMPONENT IN QUADRUPOLE MAGNETS*

W. V. Hassenzahl
Los Alamos Scientific Laboratory
University of California
Los Alamos, New Mexico

Abstract

The stringent field requirements of the beam lines at the Los Alamos Meson Physics Facility (LAMPF) restrict the $n = 6$, duodecapole component in quadrupoles to <0.1% in the integrated field. This has been achieved by the standard procedure of chamfering the poles.

An algorithm has been developed which relates the chamfer required to reduce the integrated duodecapole component to three quantities: the bore radius, the iron length, and the central field duodecapole component. Since the central field value of $n = 6$ may be calculated from the pole contour and the coil geometry, the chamfer may be prescribed before fabrication.

Equivalently, the algorithm may be used to choose a pole contour such that the central and fringe field duodecapole components cancel.

I. Introduction

Several high resolution beam lines at the Los Alamos Meson Physics Facility (LAMPF) have stringent field requirements on the bending and quadrupole magnets. TRIM and POISSON were used to optimize the pole contour to remove the duodecapole component in the central or two-dimensional region of the quadrupole magnets. To meet the field requirements, the magnitude of the nonquadrupole harmonics in the integrated field had to be kept below 0.1%. In the past, chamfers have been used at CERN and SLAC on the pole ends to reduce the integrated duodecapole component. This technique was used at LAMPF on a variety of quadrupoles having different lengths, bores, and pole contours.

An algorithm is described which may be used to specify the magnitude of chamfer required to insure a small duodecapole component in the integrated field. The size of the chamfer is determined by the iron length, the bore radius, and the duodecapole component in the two-dimensional region. The effect of field clamps or mirror plates is discussed.

II. Two-Dimensional Field Calculations

The field in the two-dimensional region of a multipole magnet may be expressed in the form

$$\vec{B}(r,\theta) = \sum_{n=0}^{\infty} B_n\left(\frac{r}{R}\right)^{n-1}[\cos(n\theta+\phi_n)\hat{r}+\sin(n\theta+\phi_n)\hat{\theta}] \quad (1)$$

where

$R = \frac{d}{2}$ is the bore radius for a quadrupole and

B_n is the field amplitude at the bore radius.

The integrated field may be expressed in an identical form[1]

$$\vec{J}(r,\Theta) = \sum_{n=0}^{\infty} J_n\left(\frac{r}{R}\right)^{n-1}[\cos(n\Theta+\phi_n)\hat{r}+\sin(n\theta+\phi_n)\hat{\theta}] \quad (2)$$

where

$$J_n = \int_{-\infty}^{\infty} B_n dz.$$

In quadrupole magnets B_2 is the major component and all other B_n are small. In the limit of perfect symmetry, only B_6, B_{10}, B_{14}...exist, and their values are determined by the pole contour and coil placement.[2] The other B_n exist in real magnets and depend on the deviations from perfect symmetry and the mechanical tolerances of assembly.

Computer programs are available which calculate the theoretical harmonic content from the output of programs such as TRIM and POISSON.[3] Due to the symmetry involved, the potentials or fields are only calculated for one quadrant or octant. Clearly the only nonzero components from a Fourier analysis of this data will be B_2, B_6, etc. The calculated harmonics have been compared with measurements for most of the magnets described, and agree to ±0.05%. Other calculations have been used to effect a small duodecapole component in the two-dimensional region.[4]

There is an out-of-phase duodecapole field associated with the ends of a quadrupole. The magnitude of this component, relative to the central field gradient, depends only on the end geometry of the magnet.

III. Measurement Techniques

The values of B_n and J_n, Eqs. (1) and (2), are obtained by step-rotating coils[5] in the bore of a quadrupole. In the step-rotated technique the output of the coil is fed to an integrator which is in turn connected to a DVM. At evenly spaced angular intervals the output of the integrator is read and stored on magnetic tape for analysis. The results of this type of measurement have been checked against a continuously rotating coil of the type described by Cobb et al.[6,7] A typical coil configuration is shown in Fig. 1.

*Work performed under the auspices of the U. S. Atomic Energy Commission.

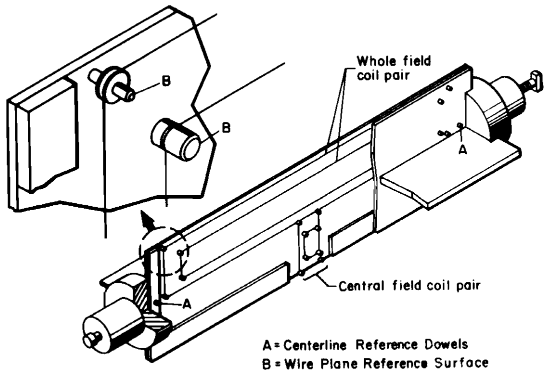

Fig. 1. Coil configuration for measuring integral and central field harmonic content in quadrupole magnets.

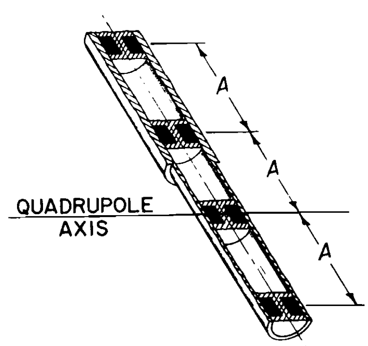

Fig. 2. Coil configuration for measuring harmonic content in quadrupole magnets as a function of axial position.

A second type of coil geometry consisting of four small, point coils[8] arranged in a bucking configuration, Fig. 2, has been used to measure gradient and harmonic content as a function of position along the magnet axis. The results of the two different types of measurements are also in agreement to ±0.05%. Using several different coils the harmonic values may be determined at different radii. The quadrupole component from a magnet discussed later is plotted at two different radii in Fig. 3. This type of information is useful in detailed studies of the fringe field effect on particle trajectories.[9]

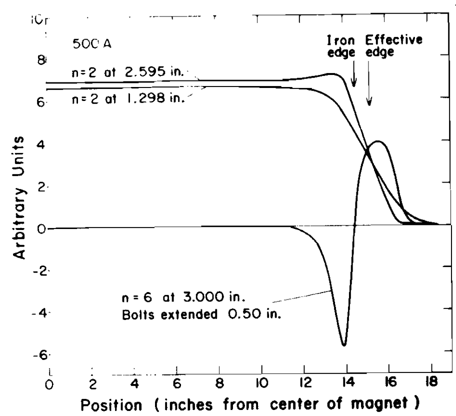

Fig. 3. Axial variation of B_2 and B_6. B_2 was measured at two different radii.

IV. Removal of Duodecapole in the Integrated Field

Techniques Available

The field variation at the square pole end of a quadrupole always introduces a duodecapole component which is 180° out of phase with respect to the quadrupole field. At least four techniques have been successfully used to cancel the end field effect.

A. The square pole end may be rounded or chamfered as in Fig. 7.

B. A field clamp may be used[1] with adjustable bolts positioned in the plane which is an extension of the midplane of each pole.

C. A pole contour may be chosen which intentionally introduces a duodecapole component to cancel the fringe field component. This technique is particularly effective where space limitations restrict magnet length.[10]

D. A technique similar to the chamfer is to introduce a shim on the flat end of the pole. This has the advantage of increasing rather than decreasing effective length which may be important on short magnets in cramped quarters.[11]

The first technique has been used extensively at LAMPF to improve the quality of quadrupole magnets. Both the first and second techniques were used on one set of quadrupoles which have unusually high field quality requirements over a large field range. The exceptional results of this combination of techniques is described later.

Prototype Magnets

Several small prototype magnets were fabricated at Los Alamos to test the effectiveness of mineral-insulated cable as a conductor. These magnets were also used for pole contour, side shim, end shim, and end chamfer studies.[12,13]

The pole contour on the first 6Q22 (6 in. bore, 22 in. length) quadrupole was not optimized to eliminate B_6, the duodecapole component in the central field region. Ideally, if not zero, B_6 should be in phase with the central quadrupole field. However, on the 6Q22, the duodecapole component was -0.4% (0.4% out of phase with respect to the gradient). A small cylindrical field clamp was used on this magnet.

Several small chamfers were made on this first magnet as we had no way to predict the optimum size or to know whether or not a linear extrapolation after the first measurements would be correct. The integrated duodecapole component is listed in Table I and shown in Fig. 4 for each chamfer.

TABLE I. Integrated Field Duodecapole Component in 6Q22 Magnets

Values of J_6 are in % relative to J_2 and correspond to the maximum pole tip field of 5 kG.

Chamfer (inches)*	Integrated Duodecapole 1st poles (%)	Integrated Duodecapole 2nd poles (%)
0 x 0	-0.90	-0.53
1/2 x 1/4	-0.60	-
1/2 x 1/2	-0.55	-
5/8 x 5/8	-0.47	-
3/4 x 3/4	-0.42	+0.23
7/8 x 7/8	-0.35	-
1 x 1†	-0.31	+0.32

*First value listed is distance along the axis.
†Maximum chamfer possible due to limitations of coil position.

A second set of poles were fabricated and placed in the same yoke. The only change was the pole contour. The central field duodecapole component with the new poles was +0.28%. Only two chamfers were made on this magnet. The duodecapole components in the integrated field for this pole contour are also listed in Table I and plotted in Fig. 4.

These magnets are relatively long compared to their bore; they have field clamps, and one has a large negative central field duodecapole component. These three factors made the reduction of J_6 to zero impossible on the first magnet. However, we see that the effect of the chamfer is linear over a range from 0 to 0.75 in. Larger chamfers are proportionally less effective. The maximum correction possible is about 1.0%.

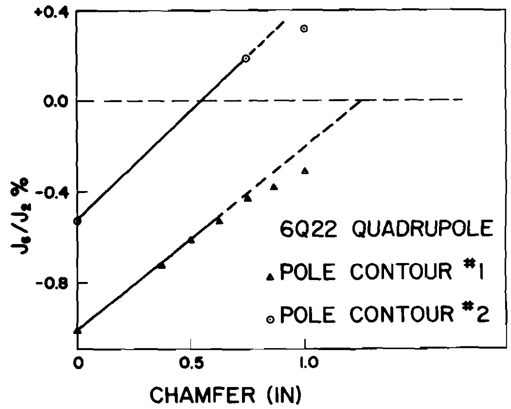

Fig. 4. Duodecapole, J_6, in 6Q22 quadrupole as a function of chamfer.

A similar series of measurements were next made on a narrow quadrupole 8QN16 with no field clamp. The results of this set of measurements were used to estimate the magnitude of chamfer required on a somewhat similar 11QN22 magnet. The results exceeded our expectations with the chamferred quadrupole having only 0.05% duodecapole in the integrated field.

V. Application to Other Magnets

The measurements on the 8QN16 and 11QN22 are shown in Fig. 5. The abcissa is the dimensionless quantity chamfer/bore diameter $\alpha = c/d$.

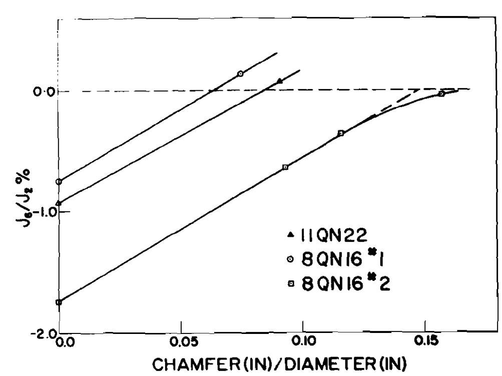

Fig. 5. Duodecapole, J_6, in 8QN16 and 11QN22 quadrupoles.

With this choice of parameter the slope of a curve only depends on two factors. The first is another dimensionless quantity, iron length/bore diameter, $\beta = \ell/d$, and the second factor is the coil geometry and whether or not a field clamp is used. For the normal range of coil design and field clamp configuration, this second factor has a small effect on the size of chamfer required. For magnets with similar values of β, and similar end geometries, the zero intersection depends only on the central field duodecapole component.

The absolute magnitude of J_6 may be expressed as

$$J_6 = B_6 \ell - C_6 + D_6 \alpha \tag{3}$$

where

C_6 is the end field contribution to the duodecapole and is proportional to B_2 up to the field level where saturation in effect rounds off the square edge.

D_6 is a measure of the effectiveness of the chamfer in changing J_6.

The value of C_6 is empirically determined to be $0.026\, B_2(G)d(in.)$. The value 0.026 may be as large as 0.029 for a magnet with a field clamp close to the pole and as small as 0.024 for magnets with large elliptical poles and the coils displaced a large distance from the bore.

Ideally, the fields in a well designed quadrupole should satisfy the two conditions $B_6 = 0$ and $J_6 = 0$. It has been difficult to attain the first condition exactly even with modern computer programs. However, measurements have been made on enough magnets to determine the chamfer required to make $J_6 = 0$ if $B_6 = 0$. This value is

$$\alpha = 0.097. \tag{4}$$

The quantity D_6 is then $D_6 = 0.097\ C_6$.

Even if $B_6 \neq 0$ it is still possible on most magnets to find a chamfer to make $J_6 = 0$. Setting $J_6 = 0$ and solving Eq. (3) for α:

$$\alpha = 0.097 - 3.77\, \beta \frac{B_6}{B_2} \tag{5}$$

Some consideration must be given to the following factors in using this formula:

A. For very high fields a slightly larger chamfer may be required, 5% or 10% larger.

B. If a field clamp is used a slightly larger chamfer will be required, again 5% or 10% larger.

C. For a quadrupole with very wide poles, e.g., a magnet in which an elliptical beam can go to a distance of 1.5 R between the pole faces, a smaller than predicted chamfer will be required.

Since the effective length of a quadrupole is reduced in the process of chamfering the pole end, it will be desirable in some cases to remove the integrated duodecapole component without using a chamfer. This may be accomplished by properly choosing B_6 to cancel the fringe field effects.

Setting $J_6 = 0$ and $\alpha = 0$ in Eq. (3),

$$\frac{B_6}{B_2} = \frac{0.026}{\beta} \tag{6}$$

This relationship will be most useful for very short magnets where space or maximum field requirements are more important than field quality.

Measurements on the 6Q29

The beam line leading to the high resolution proton spectrometer (HRS) at LAMPF has particularly high field quality requirements. One set of nine quadrupoles, the twister quads, used to rotate the x and y phase space were measured extensively. For later comparison the harmonic content in the quadrupole as received is listed in Tables II and III.

Table II. Central Field Harmonic Content in Twister Quadrupole 6Q29

Note the very low values for all harmonics, indicating good design and tight manufacturing tolerance.

Current (Amps)	$\frac{B_2}{d}$ (kG/in.)	$\frac{B_3}{B_2}$ (%)	$\frac{B_6}{B_2}$ (%)	$\frac{B_{10}}{B_2}$ (%)
900	2.410	0.22	0.03	0.10
600	1.796	0.03	0.03	0.07
400	1.203	0/02	0.02	0.06
200	0.607	0.02	0.03	0.08

Table III. Integrated Field Harmonic Content in Twister Quadrupole 6Q29

Data are for no chamfer, bolts extended 0.5 in. and field clamp 0.75 in. closer to pole than in Fig. 7.

Current (Amps)	$\frac{J_2}{d}$ (kG)	$\frac{J_3}{J_2}$ (%)	$\frac{J_6}{J_2}$ (%)	$\frac{J_{10}}{J_2}$ (%)
900	72.1	0.25	0.83	0.05
600	54.1	0.05	0.78	0.04
400	36.2	0.05	0.71	0.05
200	18.3	0.05	0.67	0.06

Our goal was to reduce the duodecapole component to <0.1% over a range of currents from 200 to 900 A; the maximum was later reduced to 800 A. Since the pole contour was optimized to reduce B_6 to zero, we would have been able to predict the chamfer required except that we could not calculate the effect of the bolts as a trim adjustment on J_6.

A series of measurements were made on the first twister quad with different chamfers, field clamp positions, and bolt extension. The values of J_6 as a function of chamfer size for two different bolt configurations are plotted in Fig. 6. Data from the two 6Q22 magnets are plotted for comparison. A cross section of the final configuration of the end of the 6Q29 is shown in Fig. 7.

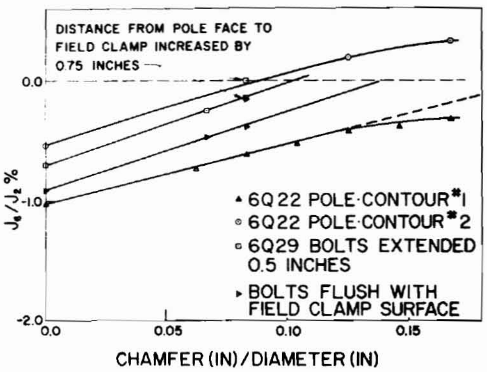

Fig. 6. Duodecapole, J_6, in 6Q29 and the two 6Q22 quadrupoles. Two different bolt configurations are plotted for the 6Q29.

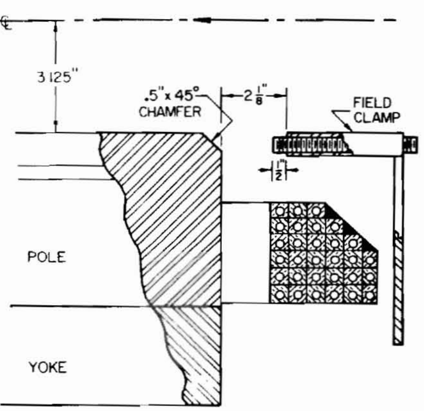

Fig. 7. Optimized end configuration for 6Q29. This geometry minimizes J_6 for all currents.

The harmonic content for this configuration is listed in Table IV. Although J_{10} increased slightly as J_6 was reduced, there is not really a problem as this component drops off as r^9. The large field clamp on this magnet does reduce the effective length by about 1 in. which should not, in general, be a problem.

Table IV. Integrated Field Harmonic Content in Twister Quadrupole 6Q29 after Trimming the End to Minimize J_6 at All Currents

End geometry is shown in Fig. 7.

Current (Amps)	$\frac{J_2}{d}$ (kG)	$\frac{J_3}{J_2}$ (%)	$\frac{J_6}{J_2}$ (%)	$\frac{J_{10}}{J_2}$ (%)
800	68.3	0.13	0.05	-0.15
600	54.5	0.04	0.03	-0.15
400	36.6	0.03	0.05	-0.16
200	18.3	0.04	0.05	-0.16

The end field geometry determined on this magnet may be scaled up or down for magnets with other diameters. This pole geometry will minimize J_6 for all pole contours with $B_6 \simeq 0$ and is recommended for all high field quality quadrupoles.

IV. Conclusion

An algorithm is presented which allows an a priori removal of the duodecapole component in the integrated field of a quadrupole magnet. The chamfer required depends on the ratio of the central field duodecapole component to the gradient, the length of the magnet, and the diameter.

A 6Q29 magnet was measured and a parameterization study was made to minimize J_6 over the complete range of currents. The end field geometry determined in this study should be used to minimize the integrated duodecapole component on any magnet with $B_6 \simeq 0$.

References

1. K. Halbach, private communication.
2. K. Halbach, Nucl. Instr. Methods 74, 147 (1969).
3. The program HARMAL developed at LAMPF for harmonic analysis of data from quadrupole magnets has been modified to calculate harmonics from the fields calculated by TRIM. R. Yourd, LBL, Berkeley, Ca, wrote a program MINT which Fourier analyzes the vector potentials calculated by POISSON.
4. E. Taylor, Proc. Int. Symp. on Magnet Technology, Stanford, 1965, p. 208.
5. A technique originally developed by K. Halbach at LBL. It is a powerful technique when used with a small digital computer for control and analysis.
6. J. Cobb and R. Cole, Proc. Int. Symp. on Magnet Technology, Stanford, 1965, p. 431.
7. J. Cobb, A. R. Burfine, and D. R. Jensen, Proc. Int. Conf. on Magnet Technology, RHEL, England, 1967, p. 247.
8. R. F. K. Herzog and O. Tischler, Rev. Sci. Instr. 24, 1001 (1953).
9. H. A. Thiessen, "Spectrometer Design at LASL," these proceedings.
10. R. Perin, CERN IBR-MA/70-16 and Proc. 3rd Int. Conf. on Magnet Technology, DESY, Hamburg, 1970.
11. A. Asner, CERN, "The End Field Compensation of Iron Contour Quadrupoles."
12. A. Harvey and R. D. Turner, Proc. Particle Ac. Conf., Chicago, 1971, IEEE Trans. Nucl. Sci. NS-18, No. 3, 892 (1971).
13. A. Harvey, "Radiation-Hardened Magnets Using Mineral-Insulated Conductors," these proceedings